Geophysical Journal International

Geophys. J. Int. (2024) **238,** 820–826
Advance Access publication 2024 June 06
GJI Seismology

https://doi.org/10.1093/gji/ggae185

Deformation of solid earth by surface pressure: equivalence between Ben-Menahem and Singh's formula and Sorrells' formula

Toshiro Tanimoto

Earth Research Institute and Department of Earth Science, University of California, Santa Barbara, CA 93106*, USA. E-mail: toshiro@geol.ucsb.edu*

Accepted 2024 May 22. Received 2024 May 19; in original form 2024 January 12

SUMMARY

Atmospheric pressure changes on Earth's surface can deform the solid Earth. Sorrells derived analytical formulae for displacement in a homogeneous, elastic half-space, generated by a moving surface pressure source with speed c. Ben-Menahem and Singh derived formulae when an atmospheric P wave impinges on Earth's surface. For a P wave with an incident angle close to the grazing angle, which essentially meant a slow apparent velocity c_a in comparison to P- (α') and S-wave velocities (β') in the Earth ($c_a \ll \beta' < \alpha'$), they showed that their formulae for solid-Earth deformations become identical with Sorrells' formulae if c_a is replaced by c. But this agreement was only for the asymptotic cases ($c_a \ll \beta'$). The first point of this paper is that the agreement of the two solutions extends to non-asymptotic cases, or when c_a/β' is not small. The second point is that the angle of incidence in Ben-Menahem and Singh's problem does not have to be the grazing angle. As long as the incident angle exceeds the critical angle of refraction from the P wave in the atmosphere to the S wave in the solid Earth, the formulae for Ben-Menahem and Singh's solution become identical to Sorrell's formulae. The third point is that this solution has two different domains depending on the speed c (or c_a) on the surface. When c/β' is small, deformations consist of the evanescent waves. When c approaches Rayleigh-wave phase velocity, the driven oscillation in the solid Earth turns into a free oscillation due to resonance and dominates the wavefield. The non-asymptotic analytical solutions may be useful for the initial modelling of seismic deformations by fast-moving sources, such as those generated by shock waves from meteoroids and volcanic eruptions because the condition $c/\beta' \ll 1$ may be violated for such fast-moving sources.

Key words: Seismic noise; Surface waves and free oscillations; Theoretical seismology; Wave scattering and diffraction.

1 INTRODUCTION

Deformations in the solid Earth, caused by an incident atmospheric P wave on Earth's surface can be observed commonly now because of the availability of seismic stations with co-located pressure and seismic sensors. An example is the EarthScope network after 2011 (e.g. Tytell *et al.* 2016). However, such a solid-Earth deformation by atmospheric pressure has been analysed since the 1960s. For example, Sorrells (1971), Sorrells *et al.* (1971) and Sorrells & Goforth (1973) analysed co-located pressure and seismic data and demonstrated the existence of wind-related seismic noise.

Other recent examples include volcano monitoring from infrasound signals and ground deformation (Ichihara *et al.* 2012; Nishida & Ichihara 2016), ground deformation caused by shock waves from Space Shuttles (Kanamori *et al.* 1991, 1992) and meteoroid falls (Langston 2004; Edwards *et al.* 2007, 2008), seismic deformations caused by thunder (Lin & Langston 2007), and seismic noise generated by airplanes and helicopters (Meng & Ben-Zion 2018).

Many of these studies relied on the theory of Ben-Menahem & Singh (1981) for the modelling of seismic signals (Fig. 1a). We refer to this book as BS81, hereafter. More specifically, we refer to section 9.4.3. in BS81. In their problem, the atmosphere was a homogeneous half-space with P-wave velocity α, and the solid Earth was also a homogenous half-space with P-wave velocity α' and S-wave velocity β'. We use a prime to indicate a parameter in the solid Earth.

When an incident atmospheric P wave impinges on the surface (Fig. 1a), the solid Earth deforms. For the grazing incidence of atmospheric P waves, Ben-Menahem & Singh (1981) showed that the formulae for a plane-wave solution can be written

$$U_z = -\frac{c_a}{2\omega\mu'}\frac{\lambda'+2\mu'}{\lambda'+\mu'}P_0(\omega)e^{i\omega(t-x/c_a)}, \quad (1)$$

$$U_x = -\frac{ic_a}{2\omega(\lambda'+\mu')}P_0(\omega)e^{i\omega(t-x/c_a)}, \quad (2)$$

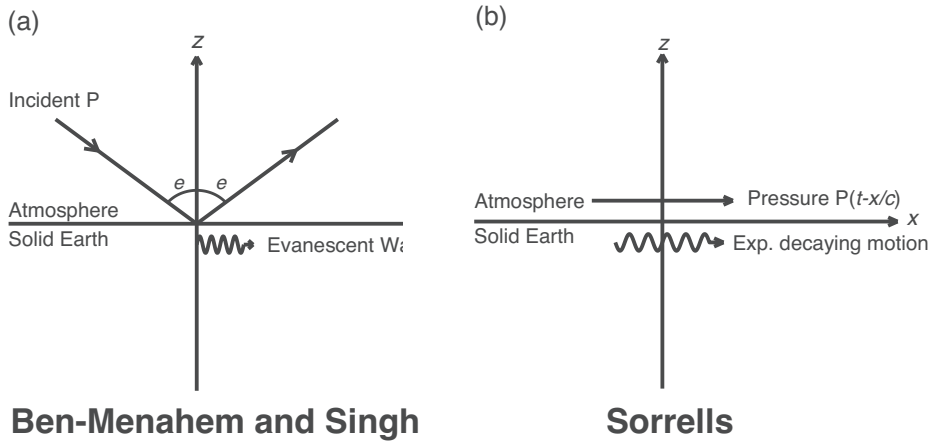

Figure 1. (a) The problem posed by Ben-Menahem and Singh (1981). The illustration is for a case of the post-critical incident angle e. Ray-theoretically, the total reflection occurs and the evanescent waves are generated in the solid Earth. Our sign convention for displacement is upwardly positive. (b) The problem posed by Sorrells (1971). The wind-related pressure source moves on the Earth's surface with speed c, generating decaying motion from the surface in the negative z-direction. There is no decay in the x-direction.

where U_z and U_x are vertical and horizontal displacements, ω is an angular frequency, t is time, c_a is phase velocity along the surface (the x-axis in Fig. 1), λ' and μ' are Lame's constant and shear modulus in the solid Earth and $P_0(\omega)$ is the Fourier amplitude of surface pressure at an angular frequency ω. Eqs (1) and (2) are the same as (9.187) in BS81 and are asymptotic solutions, derived under the condition $c_a \ll \beta' < \alpha'$. Since $\beta' < \alpha'$ always holds, we simply refer to this asymptotic condition as $c_a \ll \beta'$ or $c_a/\beta' \ll 1$.

Sorrells (1971) derived formulae for deformation in the solid Earth generated by a moving pressure source on the Earth's surface (Fig. 1b). He also assumed a homogeneous half-space for the solid Earth. Denoting the velocity of this pressure source by c, surface displacements are given by

$$U_z = -\frac{c}{2\omega\mu'}\frac{\lambda'+2\mu'}{\lambda'+\mu'}P_0(\omega)e^{i\omega(t-x/c)}, \tag{3}$$

$$U_x = -\frac{ic}{2\omega(\lambda'+\mu')}P_0(\omega)e^{i\omega(t-x/c)}, \tag{4}$$

where we use the convention that vertical displacement is positive upward. Sorrells (1971) used the opposite sign convention. Sorrells (1971) derived these formulae (eqs 23 and 24 in Sorrells, 1971) under the asymptotic condition $c/\beta' \ll 1$. In his problem, since surface pressure is related to wind, c was close to wind speed. Wind speed is typically in the range of 0–20 m s^{-1} (e.g. Tanimoto & Wang 2019) and is much smaller than P- (α') and S-wave velocities (β') in the solid Earth.

If we put $c_a = c$, eqs (1) and (2) are the same with eqs (3) and (4). This equality was pointed out in BS81.

The first point of this paper is that this equality holds, even when c/β' is not small. The agreement of solutions extends to non-asymptotic cases whose c can be any value within the range $0 \le c < \beta'$. We will sketch the derivation steps in Section 2. The upper limit arises because of the condition that the incident angle of P waves has to be larger than the critical angle of refraction.

The second point is that this agreement is not limited to the case of grazing-angle incidence for the P-wave incidence problem (BS81). The formulae for an incident angle larger than the critical angle are the same as with Sorrells' solutions.

In Section 3, we will show that this identical solution has two principal domains, depending on the speed c (or c_a). When c/β' is small, deformations in solid Earth consist of the evanescent waves. When c becomes large and approaches the Rayleigh-wave phase velocity, the evanescent waves turn into a free oscillation due to resonance and Rayleigh waves become dominant in the wavefield. This is the third point of this paper. However, most phenomena that have been reported (e.g. Ichihara *et al.* 2012; Kanamori *et al.* 1991, 1992) were in the evanescent-wave domain.

In Section 4, we will discuss three points. The first point is on the validity of non-asymptotic solutions. If the P-wave velocity in the atmosphere is higher than the S wave in the solid Earth, the agreement of solutions cannot occur. Also, in such a medium there is a possibility of the emergence of air-coupled Rayleigh waves (Press & Ewing 1951; Ewing *et al.* 1957). The simple two-homogeneous half-space model of this paper cannot model such signals, although observations of air-coupled Rayleigh waves are real at stations in a sedimentary region (Langston 2004; Edwards *et al.* 2007, 2008). The second point of discussion is the misuse of the term 'pressure-induced surface waves' in BS81 for the evanescent waves. These evanescent waves are not surface waves because their phase velocity (c_a) is determined by the apparent velocity of the incoming P wave and is not equal to the Rayleigh-wave phase velocity. The third point is on the extension of the solutions to the range $c/\beta' > 1$, the supershear case of c. This problem is complicated due to the possibility of the development of shock fronts.

In Section 5, we summarize our conclusions. Despite some deficiencies, the non-asymptotic formulae in this paper may be useful for the initial study of shock-wave-induced deformations, as the formulae remain valid for fast-moving pressure sources.

2 DERIVATION OF NON-ASYMPTOTIC SOLUTIONS

In this section, we summarize the main steps of derivation for the non-asymptotic solutions. The main point is that the formulae for a post-critical-angle case for the P-wave incidence problem in BS81 have the same form as the formulae for the moving pressure problem by Sorrells (1971), even when c/β' is not small. These non-asymptotic formulae are eqs (18) and (21).

2.1 Formulae for the case of incident *P* waves

In the problem of BS81, an incident *P* wave from the atmosphere makes an angle e when it reaches the Earth's surface (Fig. 2). This incident wave creates a reflected *P* wave, a refracted *P* wave (P') and a refracted *S* wave (S'). The angles associated with these waves e, e' and f' are defined in the figure. These notations, as introduced by BS81, may differ from standard seismological conventions but we follow their notations closely and build on their derivation steps.

We seek a plane-wave solution and assume that each term is proportional to $e^{i(\omega t - kx)}$, where k is a wavenumber. This wave propagates with phase velocity c_a in the x-direction given by $c_a = \omega/k$. A solution for a more complicated time-dependent case can be obtained by taking a linear superposition of Fourier components.

By Snell's law, we have

$$c_a = \frac{\alpha}{\sin(e)} = \frac{\alpha'}{\sin(e')} = \frac{\beta'}{\sin(f')}, \tag{5}$$

where phase velocity c_a in the x-direction remains constant through the reflection and refraction at the boundary. From eq. (5), we can write

$$\sin(e') = \frac{\alpha'}{c_a}, \tag{6}$$

$$\sin(f') = \frac{\beta'}{c_a}. \tag{7}$$

When e is smaller than the critical angle of reflection, we can write

$$\cos(e') = \sqrt{1 - (\alpha'/c_a)^2}, \tag{8}$$

$$\cos(f') = \sqrt{1 - (\beta'/c_a)^2}, \tag{9}$$

but when it is larger than the critical angle, they become (eq. 9.182 in BS81)

$$\cos(e') = -i\sqrt{(\alpha'/c_a)^2 - 1}, \tag{10}$$

$$\cos(f') = -i\sqrt{(\beta'/c_a)^2 - 1}, \tag{11}$$

they become purely complex numbers. The minus signs on the right-hand side arise because of the regularity condition as $z \to -\infty$. Using eqs (10) and (11) is essential to include the diffraction effects. The agreement of solutions between BS81 and Sorrells occurs when eqs (10) and (11) are used.

Because of the large contrast between the atmospheric *P*-wave velocity and the seismic-wave velocities in solid Earth, the critical angles for refraction are generally quite small. Table 1 shows two examples; the first case is when atmospheric *P* waves are incident on a hard-rock site (case 1: $\alpha' = 6\ \mathrm{km\,s^{-1}}$ and $\beta' = 3.5\ \mathrm{km\,s^{-1}}$) and the second case is when *P* waves are incident on a sedimentary rock site (case 2: $\alpha' = 2\ \mathrm{km\,s^{-1}}$ and $\beta' = 1\ \mathrm{km\,s^{-1}}$). The table shows that even with a slower *S*-wave speed ($1\ \mathrm{km\,s^{-1}}$) in case 2, the critical angle of refraction to S' wave is about 20° (19.88°). For a hard-rock site ($\beta' = 3.5\ \mathrm{km\,s^{-1}}$), the critical angle to S'-wave refraction occurs at 5.57°. Therefore, it is common to encounter a situation where the incident angle exceeds the critical angle.

We note that having an incident *P* wave is equivalent to having the surface pressure (BS81)

$$P(\omega) = P_0(\omega)\exp^{i\omega(t - x/c_a)}, \tag{12}$$

where

$$P_0(\omega) = \frac{2\rho\alpha m_1}{m_1 + m_2} \tag{13}$$

with

$$m_1 = \cos(e)\left[\left(\frac{\beta'}{\alpha'}\right)^2 \sin(2e')\sin(2f') + \cos^2(2f')\right], \tag{14}$$

$$m_2 = \frac{\rho\alpha}{\rho'\alpha'}\cos(e'). \tag{15}$$

Using this pressure formula, a formula for the ratio between vertical displacement and surface pressure becomes (BS81)

$$\frac{U_z(\omega)}{P(\omega)} = i\frac{m_2\cos(e)}{\omega\rho\alpha m_1}, \tag{16}$$

where $U_z(\omega)$ is the Fourier spectra of vertical displacement. Here, we modified their eq. (9.181) for the vertical component from velocity to displacement.

Substituting eqs (14) and (15) into eq. (16), we get

$$\frac{U_z(\omega)}{P(\omega)} = \left(\frac{i}{\omega\rho'\alpha'}\right)\frac{\cos(e')}{\left(\frac{\beta'}{\alpha'}\right)^2 \sin(2e')\sin(2f') + \cos^2(2f')}. \tag{17}$$

Using eqs (6), (7), (10) and (11) and noting that

$$\sin(2e')\sin(2f') = -4\frac{\alpha'^2\beta'^2}{c_a^4}\sqrt{1 - \frac{c_a^2}{\alpha'^2}}\sqrt{1 - \frac{c_a^2}{\beta'^2}},$$

$$\cos^2(2f') = \left(1 - 2\frac{\beta'^2}{c_a^2}\right)^2.$$

we get

$$U_z(\omega) = \frac{c_a}{\omega\mu'}\frac{\xi_{\alpha'}\left(1 - \xi_{\beta'}^2\right)}{\left(1 + \xi_{\beta'}^2\right)^2 - 4\xi_{\alpha'}\xi_{\beta'}}P(\omega), \tag{18}$$

where we defined

$$\xi_{\alpha'} = \sqrt{1 - \frac{c_a^2}{\alpha'^2}}, \tag{19}$$

$$\xi_{\beta'} = \sqrt{1 - \frac{c_a^2}{\beta'^2}}. \tag{20}$$

Similarly, by starting from the horizontal formula (9.181) in BS81, we obtain the horizontal displacement in the direction of propagation (the x-axis)

$$U_x(\omega) = \frac{ic_a}{\omega\mu'}\frac{\left(1 + \xi_{\beta'}^2\right) - 2\xi_{\alpha'}\xi_{\beta'}}{\left(1 + \xi_{\beta'}^2\right)^2 - 4\xi_{\alpha'}\xi_{\beta'}}P(\omega). \tag{21}$$

There is an important feature to be noted in the non-asymptotic formulae (18) and (21). That is, they are valid as long as eqs (10) and (11) are used. It means that they are valid when the *P*-wave incident angle is larger than the critical angle of refraction from the *P* wave in the atmosphere to the *S* wave in the solid Earth. Also, because the incident angle is required to be larger than the critical angle, the range of c_a is $0 < c_a \leq \beta'$ for the non-asymptotic solutions.

It may also be noted that eqs (18) and (21) will not be realized if β' is smaller than the *P*-wave velocity in the atmosphere because the critical angle does not exist in such a case. Such a situation may occur in a region with low-velocity sediment where β' may become as low as 100–200 $\mathrm{m\,s^{-1}}$ (Langston 2004; Edwards *et al.* 2007, 2008).

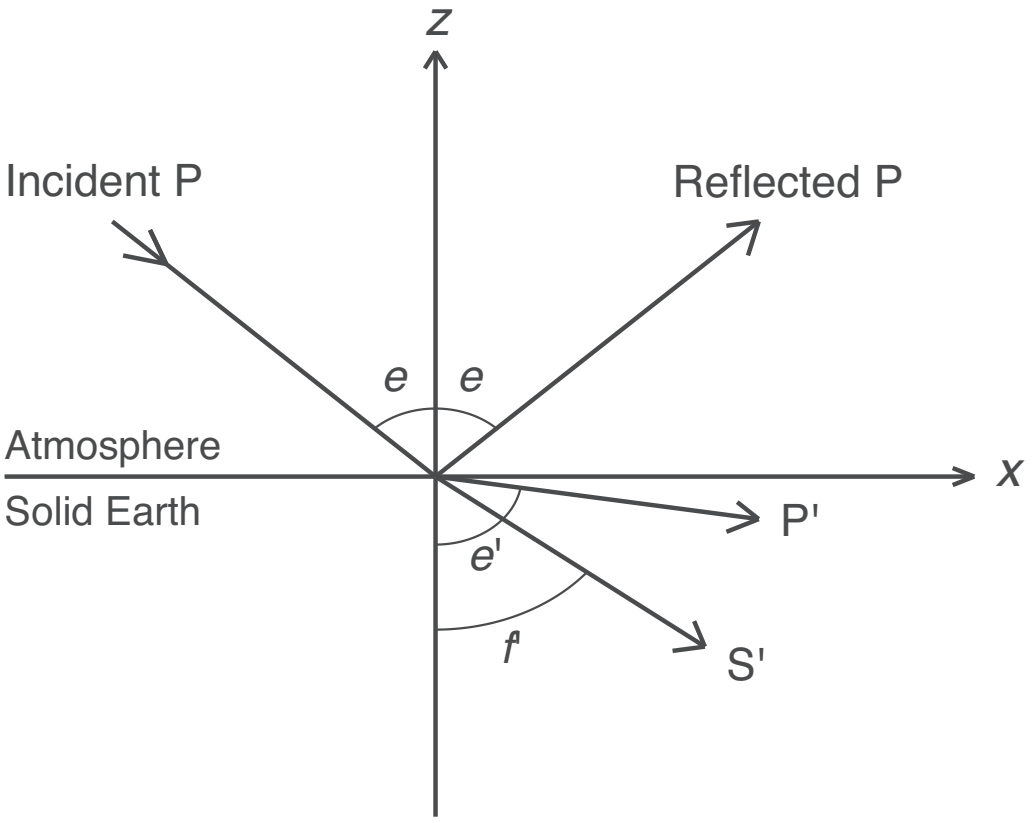

Figure 2. Definition of angles. The z-axis is upwardly positive.

Table 1. Examples of critical angles. P-wave velocity in the atmosphere is 340 ($m\,s^{-1}$). Case 1 (hard-rock site) and case 2 (sedimentary rock site) have different P- and S-wave velocities in the solid Earth.

Case	P wave ($m\,s^{-1}$)	S wave ($m\,s^{-1}$)	P' critical angle	S' critical angle
1	6000	3500	3.25^o	5.57^o
2	2000	1000	9.79^o	19.88^o

2.2 Formula for the case of moving surface pressure source

Sorrells (1971) derived formulae for deformation in the solid Earth, generated by a moving pressure source on the surface with speed c (Fig. 1b). Extension to a multilayered case is straightforward (Tanimoto & Wang, 2019) but in this paper, we stick to a case of homogeneous elastic half-space. The derivation in this paper is essentially the same not only with Sorrells (1971) but also with Lamb (1904), although Lamb (1904) examined the case of a point pressure source. Here, we are concerned about a loading pressure source that is spread out on the surface and moving in time.

The solution can be obtained by starting with the displacement potentials for the P waves (ϕ) and S waves (Ψ) as

$$\mathbf{u} = \nabla\phi + \nabla \times \nabla \times (0, 0, \Psi), \tag{22}$$

where ϕ and Ψ satisfy the equations

$$\frac{\partial^2\phi}{\partial t^2} = \alpha'^2\nabla^2\phi, \tag{23}$$

$$\frac{\partial^2\Psi}{\partial t^2} = \beta'^2\nabla^2\Psi. \tag{24}$$

One of the boundary conditions is that a solution must decay as $z \to -\infty$. We also have the stress boundary conditions at the surface, which can be expressed by $\sigma_{xz} = 0$ and $\sigma_{zz} = -P$. For this problem, we seek a plane-wave solution.

Regularity of displacements as $z \to -\infty$ requires us to choose a solution which has the form $\phi = Ae^{\nu_{\alpha'}z}$ and $\Psi = Be^{\nu_{\beta'}z}$ where $\nu_{\alpha'} = \sqrt{k^2 - \omega^2/\alpha'^2}$ and $\nu_{\beta'} = \sqrt{k^2 - \omega^2/\beta'^2}$. The coefficients A and B are determined from the two boundary conditions at the surface. This leads to two equations given by

$$2\nu_{\alpha'}A + \left(2k^2 - \frac{\omega^2}{\beta'^2}\right)B = 0, \tag{25}$$

$$\left[-\lambda'\frac{\omega^2}{\alpha'^2} + 2\mu'\left(k^2 - \frac{\omega^2}{\alpha'^2}\right)\right]A + 2\mu'k^2\nu_{\beta'}B = -P. \tag{26}$$

Solving for A and B, we get

$$A = \frac{2k^2 - \frac{\omega^2}{\beta'^2}}{D}P, \tag{27}$$

$$B = -\frac{2\nu_{\alpha'}}{D}P, \tag{28}$$

where

$$D = 4\mu'k^2\nu_{\alpha'}\nu_{\beta'} + \left[(\lambda' + 2\mu')\frac{\omega^2}{\alpha'^2} - 2\mu'k^2\right]\left(2k^2 - \frac{\omega^2}{\beta'^2}\right), \tag{29}$$

and the characteristic equation of Rayleigh waves for a homogeneous half-space is given by $D = 0$.

Formulae for the vertical and horizontal displacements become

$$U_z = \nu_{\alpha'} A + k^2 B = -\frac{\nu_{\alpha'}\omega^2}{\beta'^2 D} P, \tag{30}$$

$$U_x = -ikA - ik\nu_{\beta'} B = i\frac{2k\nu_{\alpha'}\nu_{\beta'} - k\left(2k^2 - \omega^2/\beta'^2\right)}{D} P. \tag{31}$$

Substituting $k = \omega/c$, $\nu_{\alpha'} = k\xi_{\alpha'}$, and $\nu_{\beta'} = k\xi_{\beta'}$ into this formula, we get

$$U_z(\omega) = \frac{c}{\omega\mu'}\frac{\xi_{\alpha'}\left(1-\xi_{\beta'}^2\right)}{\left(1+\xi_{\beta'}^2\right)^2 - 4\xi_{\alpha'}\xi_{\beta'}} P, \tag{32}$$

$$U_x(\omega) = \frac{ic}{\omega\mu'}\frac{\left(1+\xi_{\beta'}^2\right) - 2\xi_{\alpha'}\xi_{\beta'}}{\left(1+\xi_{\beta'}^2\right)^2 - 4\xi_{\alpha'}\xi_{\beta'}} P, \tag{33}$$

where they are the same as eqs (18) and (21) if we put $c = c_a$. Under the asymptotic condition $c/\beta' \ll 1$, eqs (32) and (33) become eqs (3) and (4).

3 TWO DOMAINS IN SOLUTION: EVANESCENT WAVES VERSUS RAYLEIGH WAVES

We have shown that the formulae for the post-critical incidence of atmospheric P waves (apparent velocity c_a) are the same with those for the moving-pressure source on the surface (velocity c) if we put $c_a = c$. In this section, we examine how this horizontal speed c (or c_a) influences the deformation in the solid Earth by computing the ratio of vertical seismic amplitude to surface pressure as a function of c. The parameter range of this inquiry is wider than what was considered in BS81 and Sorrells (1971). BS81 considered the case of the grazing-angle incidence of P waves on Earth's surface and thus the speed was restricted to about $c_a = 340$ m s^{-1}. Sorrells (1971) considered wind as the excitation source of seismic noise and thus the speed of pressure source c was approximately equal to wind speed, typically in the range $0 < c < 20$ m s^{-1}. Both are special cases of non-asymptotic solutions as the non-asymptotic solutions are valid for the range $0 \le c \le \beta'$.

We compute the ratio $\omega U_z(\omega)/P$ because the explicit dependence on frequency (ω) can be removed from the formulae. The non-asymptotic and the asymptotic formulae are given by

$$\frac{\omega U_z}{P} = \frac{c}{\mu'}\frac{\xi_{\alpha'}(1-\xi_{\beta'}^2)}{(1+\xi_{\beta'}^2)^2 - 4\xi_{\alpha'}\xi_{\beta'}}, \tag{34}$$

and

$$\frac{\omega U_z}{P} = -\frac{c}{2\mu'}\frac{\lambda'+2\mu'}{\lambda'+\mu'}. \tag{35}$$

An example case was calculated for the solid medium with a P-wave velocity of 6 km s^{-1} and an S-wave velocity of 3.5 km s^{-1}, respectively, and the atmospheric P-wave velocity of 340 m s^{-1} (Fig. 3). The ratio is zero when $c = 0$. For $c > 0$, it is slightly negative but appears to be running along the zero line on the scale of the plot in Fig. 3(a).

The non-asymptotic case shows a dominant peak at about 3200 m s^{-1} which is close to the Rayleigh-wave phase velocity for the structure, 3213.7 m s^{-1}. The emergence of the dominant peak near Rayleigh-wave phase velocity means that Rayleigh waves get excited if the speed c becomes close to the phase velocity. Rayleigh waves then become dominant in the wavefields.

For the range $0 \le c \le 3000$ m s^{-1} (Fig. 3b), the deviations of the asymptotic solution from the non-asymptotic solution can be confirmed to start at about 1000 (m s^{-1}) and become very large for $c > 2500$ m s^{-1}. This behaviour suggests that the non-asymptotic formulae should be used if c exceeds about 1500 m s^{-1}. Use of the asymptotic solution for seismic data from Space Shuttle Columbia (Kanamori *et al.* 1991, 1992) is justified because $c \approx 1000$ m s^{-1}. On the other hand, Qamar (1995) reported faster shock-wave speeds of about 5–7 km s^{-1}, measured for Space Shuttle Discovery and Endeavor. However, he did not show any quantitative analysis of seismic data. The analysis of his cases would have required the use of non-asymptotic solutions. Furthermore, the range of 5–7 km s^{-1} suggests that analysis for shock waves in solid Earth may be required as this velocity likely exceeds P-wave velocity at shallow depths.

For an even smaller range $0 \le c \le 500$ m s^{-1} (Fig. 3c), the asymptotic solution becomes almost exact. The non-asymptotic solution becomes almost linear in c. Two processes within this range are indicated, the deformations caused by wind-related pressure changes (e.g. Sorrells 1971) and the infrasound velocity (340 m s^{-1}).

4 DISCUSSION

4.1 Validity of the non-asymptotic equations

Because of the differences in the posed questions between BS81 and Sorrells (1971), the equivalence of the asymptotic formulae between the grazing-angle-incident case of BS81 and Sorrell's problem was a surprise when it was pointed out in BS81. In hindsight, this equivalence may not be surprising for the grazing-angle incidence of atmospheric P waves. Since P waves have pressure changes along their paths, the grazing-angle incidence case could be treated as a surface boundary-value problem instead of a wave reflection–refraction problem.

The validity of the non-asymptotic formulae for the P-wave incidence problem is not limited to the grazing-angle case. As we discussed in Section 2.1, when the incident angle e is between the critical angle θ_c ($= \sin^{-1}(\alpha/\beta')$) and 90°, the formulae have the same forms. The range of angles is indicated by stripes in Fig. 4. It also means that the formal solution for the P-wave incident problem (BS81) includes the solution for a moving surface pressure problem (Sorrells 1971) as its end-member case when $e = 90°$, although the pressure-source speed was different in each problem (340 m s^{-1} versus 1–20 m s^{-1}).

The non-asymptotic solutions may be useful for the initial modelling of seismic signals caused by fast-moving pressure sources, such as shock waves from meteoroids from outer space (e.g. Langston 2004; Edwards *et al.* 2007, 2008) and volcanic eruptions (Ichihara *et al.* 2012) because c may not be a small perturbation of S-wave velocity in the solid half-space. The speed of pressure sources can be beyond the linear range covered by the asymptotic solutions.

However, there are some sites with very slow near-surface S-wave velocity that is lower than 340 m s^{-1} (e.g. Langston 2004), especially in an area of thick sedimentary layers. The application of a simple two-half-space model of this paper fails in such a case. Furthermore, there may be an emergence of air-coupled Rayleigh waves in such a low-velocity medium. Press & Ewing (1951) showed that air-coupled Rayleigh waves can exist if the Rayleigh-wave phase velocity in the solid medium is close to the P waves in the atmosphere.

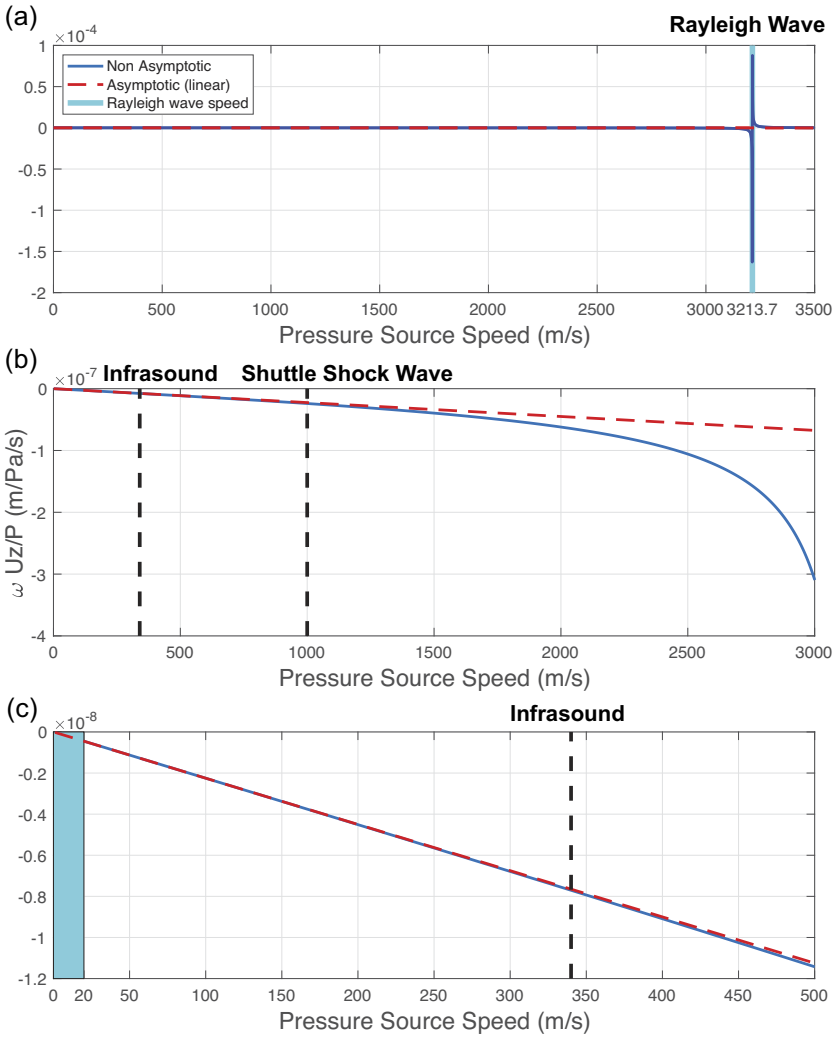

Figure 3. (a) Ratio $\omega U_z/P$ as a function of the pressure-source speed c. The range of c is $0 \le c \le 3500\ \mathrm{m\,s^{-1}}$ $(= \beta')$. The non-asymptotic solution is in dark blue and the asymptotic solution is in red dashes. The asymptotic solution is a linear line. Rayleigh-wave phase velocity is $3213.7\ \mathrm{m\,s^{-1}}$, shown by the vertical light blue line. (b) Same result for the range $0 \le c \le 3000\ \mathrm{m\,s^{-1}}$. Two vertical dashed lines are at $340\ \mathrm{m\,s^{-1}}$ (Infrasound) and $1000\ \mathrm{m\,s^{-1}}$ (Shuttle Shock Wave). (c) Same result for the range $0 \le c \le 500\ \mathrm{m\,s^{-1}}$. A typical range of wind speed ($0 < c < 20\ \mathrm{m\,s^{-1}}$) is indicated by a box.

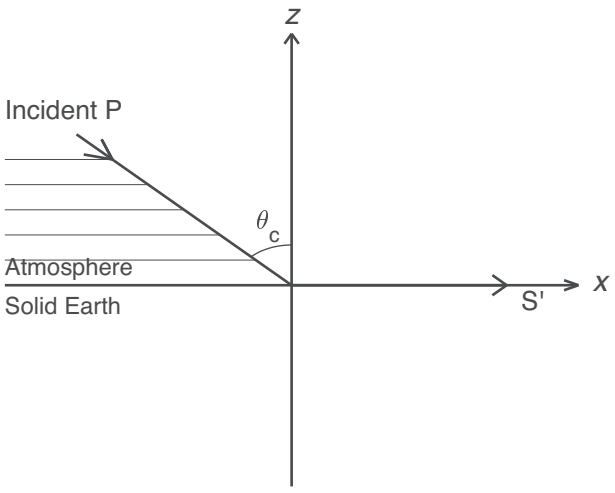

Figure 4. The non-asymptotic solutions for an incident angle larger than the critical angle $\theta_c = \sin^{-1}(\alpha/\beta')$ (the striped range) are the same with the solutions for a moving pressure source on the surface.

In addition, some complex wave phenomena in a thick sedimentary basin, such as reverberations of seismic waves in shallow layers were reported by Langston (2004) and Edwards *et al.* (2007, 2008). For such phenomena, the solutions in this paper are not useful as the assumed medium is too simple.

Nonetheless, the non-asymptotic solutions may be useful at stations in hard-rock sites. They can allow us to quickly estimate the speed of pressure sources from meteoroids and volcanic eruptions.

4.2 Evanescent waves are not surface waves

We believe that the term 'pressure-induced surface waves' in BS81 (the title of section 9.4.3) is not consistent with the conventional seismological use of the term 'surface waves'. As the analysis in Section 3 showed, when the pressure source speed c is small, deformations in solid Earth consist of evanescent waves. They are not surface waves because their phase velocity c is equal to the apparent velocity of the incoming atmospheric P waves and is different from

the phase velocity of Rayleigh waves. Generally, the amplitudes of evanescent waves are small because they are related to diffraction effects. Only when the pressure-source speed c becomes close to the Rayleigh-wave phase velocity, does the excitation of Rayleigh waves occur as the results in Fig. 3(a) show.

4.3 Super-shear case

We have not discussed a case when the surface pressure speed c exceeds S-wave velocity β' in the solid Earth. In such a case, there is a possibility of generating the cone-shaped shock front as the pressure source moves with a super-shear speed c. The formulae in this paper may still be a good approximation when the shock front is weak. But when the shock front becomes large, the analysis must include the advection term $\rho(\mathbf{v}\cdot\nabla)\mathbf{v}$ which makes the problem non-linear (e.g. Whitham 1974). Because of this complexity, an extension of the solutions to the super-shear case is not straightforward. The question is left for the future.

5 CONCLUSION

Ben-Menahem & Singh (1981) pointed out that the formulae for deformations in the solid Earth caused by an incoming P wave from the atmosphere are the same as those generated by a moving pressure source on the surface. They showed this agreement for the case of grazing-angle incidence and also under the asymptotic condition ($c \ll \beta'$).

In this paper, we derived the non-asymptotic formulae for the two problems and showed that they are equivalent in the range $0 \le c < \beta'$. We also showed that this equality was not limited to the grazing-angle case. For an incident angle beyond the critical angle, the formulae become identical to those for the moving surface-pressure source (Sorrells 1971). This identical solution has two main domains of deformation in the solid Earth. When c (or c_a) is small, the evanescent waves are generated in the solid Earth. When c becomes close to the Rayleigh-wave phase velocity, Rayleigh waves get excited and dominate the wavefield.

The asymptotic solution of Ben-Menahem and Singh has been used in many studies. Comparison of the non-asymptotic and the asymptotic solutions (linear in c) shows that the valid range of asymptotic solution is $c < 1500\ \mathrm{m\,s^{-1}}$. We found that most applications were within this valid range; for example, $c < 20\ \mathrm{m\,s^{-1}}$ for wind-related seismic noise (Wang & Tanimoto 2020, 2022), $c = 340\ \mathrm{m\,s^{-1}}$ for the infrasound signals from volcanic eruptions (Ichihara *et al.* 2012), and $c \approx 1000\ \mathrm{m\,s^{-1}}$ for shock-wave caused deformations from Space Shuttles (Kanamori *et al.* 1991, 1992).

ACKNOWLEDGMENTS

I thank Dr Adam Ringler and an anonymous reviewer for their comments that helped improve this paper. This research was supported by the SCEC matching fund at UC Santa Barbara and a fellowship from the John Simon Guggenheim Foundation.

DATA AVAILABILITY

This is an entirely theoretical work. No new data were generated or analysed in this research.

REFERENCES

Ben-Menahem, A. & Singh, S.J., 1981. *Seismic Waves and Sources,* Springer-Verlag New York Inc.

Edwards, W.N., Eaton, D.W. & Brown, P.G., 2008. Seismic observations of meteors: Coupling theory and observations, *Rev. Geophys.,* **46,** RG4007, doi:10.1029/2007RG000253.

Edwards, W.N., Eaton, D.W., McCausland, P.J., Revelle, D.O. & Brown, P.G., 2007. Calibrating infrasonic to seismic coupling using the Stardust sample return capsule shockwave: Implications for seismic observations of meteors, *J. geophys. Res.,* **112,** B10306., doi:10.1029/2006JB004621.

Ewing, M., Jardetzky, W. & Press, F., 1957. *Elastic Waves in Layered Media,* p. 380, McGraw-Hill Publishing Co., New York.

Ichihara, M., Takeo, M., Yokoo, A., Oikawa, J. & Ohminato, T., 2012. Monitoring volcanic activity using correlation patterns between infrasound and ground motion, *Geophys. Res. Lett.,* **39,** L04304, doi:10.1029/2011GL050542.

Kanamori, H., Mori, J., Anderson, D.L. & Heaton, T.H., 1991. Seismic excitation by the space shuttle Columbia, *Nature,* **349,** 781–782. doi: 10.1038/349781a0.

Kanamori, H., Mori, J., Sturtevant, B., Anderson, D.L. & Heaton, T., 1992. Seismic excitation by space shuttles, *Shock Waves,* **2,** 89–96. doi: 10.1007/BF01415896.

Lamb, H., 1904. On the propagation of tremors over the surface of an elastic solid, *Phil. Trans. R. Soc. Lond.,* **A203,** 1–42. doi: 10.1098/rsta.1904.0013.

Langston, C., 2004. Seismic ground motions from a bolide shock wave, *J. geophys. Res.,* **109,** B12309, doi:10.1029/2004JB003167.

Lin, T.-L. & Langston, C., 2007. Infrasound from thunder: a natural seismic source, *Geophys. Res. Lett.,* **34,** B10306.doi:10.1029/2007GL030404.

Meng, H. & Ben-Zion, Y., 2018. Characteristics of airplanes and helicopters recorded by a dense seismic array near Anza California, *J. geophys. Res.,* **123,** 4783–4797. doi: 10.1029/2017JB015240.

Nishida, K. & Ichihara, M., 2016. Real-time infrasonic monitoring of the eruption at a remote island volcano using seismoacoustic cross correlation, *Geophys. J. Int.,* **204,** 748–752. doi: 10.1093/gji/ggv478.

Press, F. & Ewing, M., 1951. Ground roll coupling to atmospheric compressional waves, *Geophysics,* **16,** 416–430. doi: 10.1190/1.1437684.

Qamar, A., 1995. Space shuttle and meteoroid - tracking supersonic objects in the atmosphere with seismographs, *Seismol. Res Lett.,* **66,** 6–12. doi: 10.1785/gssrl.66.5.6.

Sorrells, G., 1971. A preliminary investigation into the relationship between long-period seismic noise and local fluctuations in the atmospheric pressure field, *Geophys. J. R. astr. Soc.,* **26,** 71–82. doi: 10.1111/j.1365-246X.1971.tb03383.x.

Sorrells, G., MacDonald, J.A., Der, Z. & Herrin, E., 1971. Earth motion caused by local atmospheric pressure changes, *Geophys. J. R. astr. Soc.,* **26,** 83–98. doi: 10.1111/j.1365-246X.1971.tb03384.x.

Sorrells, G. & Goforth, T., 1973. Low-frequency earth motion generated by slowly propagating partially organized pressure fields, *Bull. seism. Soc. Am.,* **63,** 1583–1601. doi: 10.1785/BSSA0630051583.

Tanimoto, T. & Wang, J., 2019. Theory for deriving shallow elasticity structure from colocated seismic and pressure data, *J. geophys. Res., Solid Earth,* **124,** 5811–5835. doi: 10.1029/2018JB017132.

Tytell, J., Vernon, F., Hedlin, M., de Groot Hedlin, C., Reyes, J., Busby, B., Hafner, K. & Eakins, J., 2016. The USArray transportable array as a platform for weather observation and research, *Bull. seism. Soc. Am.,* **97,** 603–619. doi: 10.1175/BAMS-D-14-00204.1.

Wang, J. & Tanimoto, T., 2020. Estimating near-surface rigidity from low-frequency noise using colocated pressure and horizontal data, *Bull seism. Soc. Am.,* **XX,** 1–11.doi:10.1785/0120200098.

Wang, J. & Tanimoto, T., 2022. Estimation of Vs30 at the EarthScope Transportable Array stations by inversion of low-frequency seismic noise, *J. geophys. Res.: Solid Earth,* **127,** e2021JB023469, doi:10.1029/2021JB023469.

Whitham, G.B., 1974. *Linear and Nonlinear Waves,* John Wiley & Sons, Inc., New York. doi: 10.1002/9781118032954.